

Cooperative Adaptive Cruise Control with Robustness against Communication Delay An Approach in the Space Domain

Zhang, Yu; Bai, Yu; Wang, Meng; Hu, Jia

DOI

[10.1109/TITS.2020.2987746](https://doi.org/10.1109/TITS.2020.2987746)

Publication date

2021

Document Version

Final published version

Published in

IEEE Transactions on Intelligent Transportation Systems

Citation (APA)

Zhang, Y., Bai, Y., Wang, M., & Hu, J. (2021). Cooperative Adaptive Cruise Control with Robustness against Communication Delay: An Approach in the Space Domain. *IEEE Transactions on Intelligent Transportation Systems*, 22(9), 5496-5507. Article 9082096. <https://doi.org/10.1109/TITS.2020.2987746>

Important note

To cite this publication, please use the final published version (if applicable).
Please check the document version above.

Copyright

Other than for strictly personal use, it is not permitted to download, forward or distribute the text or part of it, without the consent of the author(s) and/or copyright holder(s), unless the work is under an open content license such as Creative Commons.

Takedown policy

Please contact us and provide details if you believe this document breaches copyrights.
We will remove access to the work immediately and investigate your claim.

Cooperative Adaptive Cruise Control With Robustness Against Communication Delay: An Approach in the Space Domain

Yu Zhang^{1b}, Yu Bai, Meng Wang^{2b}, *Member, IEEE*, and Jia Hu^{1b}, *Member, IEEE*

Abstract—In this research, an optimal control-based Cooperative Adaptive Cruise Control (CACC) system is proposed. The proposed system is able to enforce a target time gap between platoon members and is formulated in the space domain instead of the time domain which is adopted by most optimal control-based CACC systems in the past. By having this change, its robustness against communication failure is greatly improved and thus minimum safety headway buffer is reduced which leads to better mobility. In addition, third-order vehicle dynamics are modeled into the proposed control in order to improve control precision when implemented in the field. Local stability and string stability are theoretically proven. The proposed system is evaluated by simulation. Results reveal that the proposed CACC system outperforms the state-of-the-art \mathcal{H}_∞ synthesis-based controller and linear feedback-based controller. The benefit of fuel consumption reduction ranges from 0.35% to 16.11%, while the benefit of CO₂ emission ranges from 0.48% to 12.40%. Furthermore, the proposed CACC improves local stability from 11.03% to 25.90%, and string stability by up to 23.82%. The computation speed of the proposed method is 1.26 ms (with prediction horizon as 1.5 s and resolution as 0.1 s) on a regular laptop which indicates the proposed system's potential to be applied in real-time.

Index Terms—Communication delay, cooperative adaptive cruise control (CACC), local stability, space domain, string stability.

I. INTRODUCTION

COOPERATIVE ADAPTIVE Cruise Control (CACC) [1]–[5] is one of the most important cooperative automation applications. It is able to shorten the distance

Manuscript received April 2, 2019; revised September 18, 2019, December 20, 2019, and February 16, 2020; accepted April 9, 2020. Date of publication April 29, 2020; date of current version September 1, 2021. This work was supported in part by the National Natural Science Foundation of China under Grant 71871163 and Grant 61803284, in part by the Fundamental Research Funds for the Central Universities under Grant 1600219316, in part by the Shanghai Yangfan Program under Grant 18YF1424200, and in part by the Chinese Scholarship Council (CSC) under Grant 201806260147. The Associate Editor for this article was Y. Wang. (*Corresponding author: Jia Hu.*)

Yu Zhang is with the Key Laboratory of Road and Traffic Engineering of the Ministry of Education, Tongji University, Shanghai 201804, China, and also with the Department of Transport and Planning, Delft University of Technology, 2600AA Delft, The Netherlands (e-mail: 1610734@tongji.edu.cn).

Yu Bai and Jia Hu are with the Key Laboratory of Road and Traffic Engineering of the Ministry of Education, Tongji University, Shanghai 201804, China (e-mail: baiyu@tongji.edu.cn; hujia@tongji.edu.cn).

Meng Wang is with the Department of Transport and Planning, Delft University of Technology, 2600AA Delft, The Netherlands (e-mail: m.wang@tudelft.nl).

Digital Object Identifier 10.1109/TITS.2020.2987746

between vehicles and stabilize a platoon of vehicles and thus improves transportation safety [2], fuel efficiency [6] and mobility [7]–[9].

Research on CACC mainly focuses on three aspects – decision making, communication topology, and control design. The research on decision making deals with string formation/dissolution and vehicle join/leave strategies [10], [11]. Communication topology design explores the influence of information flow topology on the performance of CACC systems [12]–[14]. Typical types of information flow topologies include predecessor following (PF), predecessor-leader following (PLF) and bidirectional (BD), among which the most commonly used topology is predecessor following (PF) [1], [5], [15], where the ego vehicle receives information only from its front vehicle. Finally, works on control design focus on enabling technologies that realize platooning [2], [16]–[22].

In terms of control design, CACC system generally falls into two categories – feedback-based design [2], [17], [18] and optimal control-based design [19], [20]. Feedback-based CACC adjusts ego vehicle's acceleration to meet a desired state (headway, time gap, etc.); while optimal control-based CACC, on the other hand, aims to achieve a certain goal (comfort, fuel efficiency, etc.) over its optimization horizon. feedback-based control is currently the most prevailing way of realizing CACC, as it is reliable and has been adopted in many other types of control systems. However, due to the complexity of vehicle dynamics, tuning feedback gains of CACC systems that ensure string stability over the entire speed spectrum is quite time consuming and sometimes not feasible at all. Furthermore, to guarantee string stability, conventional feedback-based CACC systems generally requires a minimum headway [15], [17], which compromise the benefit of throughput enhancement of CACC systems. Optimal control-based CACC does not have this problem, but was held back by its demand on computing power in the past. With the advancement of onboard computers and Electrical Control Unit (ECU), optimal control-based CACC that is compatible with the real-time application is now made possible.

Existing optimal control-based CACC systems are formulated in the time domain with variables being functions of time [15], [17]–[20], [23]–[26]. However, the time domain-based method is not always well suited for all circumstances. For instance, it is difficult to properly control a CACC platoon in curve roads if the platoon is controlled

by time domain-based methods. For a CACC platoon, vehicles should share the same/similar lateral maneuver at the same longitudinal location. If the time domain-based method is applied, however, consecutive vehicles would take the same/similar longitudinal maneuver at the same time instant. Thus, the lateral and longitudinal maneuver of the platoon would be discordant (consider the situation that the leader of a platoon has already passed the curve and is accelerating, then the rest of the platoon would pass the curve with high speed). So, the platoon controlled by time domain-based methods could not properly make through curve roads. Another example is platooning on rolling terrain. In the case that one vehicle is going downhill and the other uphill, if time domain-based methods are applied, the two vehicles would share the same/similar speed and acceleration at the same time. Due to gravity, it would waste too much fuel for the following vehicle. Worst case is when the following vehicle is a truck, enforcing the same speed might not even be feasible depending on the slope. There do exist works which take slope information into account to realize eco-driving [27], [28]. However, the mutual influence between slope profile and speed trajectory in the time domain seriously influence the efficiency of the solution. There are even chance that the solution will not converge. Another drawback of time domain-based methods is that they heavily rely on the quality of communication. Since time domain-based methods require current information, if its input is not received in real-time, controller function may be impaired. Packet loss [29] and communication delay [30] have been found greatly impacting the stability and safety of CACC platoon. Even though methods proposed to deal with communication delay can enable CACC function properly [31], these methods all confront the problem that the performance of the CACC system is heavily influenced by communication delay.

All the aforementioned shortcomings of time domain-based methods can be overcome by spaced domain-based methods, which formulate and solve problems with all variables as functions of longitudinal position, instead of time. When an optimal controller is formulated in the space domain, it is feasible to enforce the same maneuver across different vehicles at the same location. Hence, CACC platoon would be able to make through curve/hilly roads. Moreover, in the space domain, the mutual influence of slope/curve profile and speed trajectory are de-coupled (speed trajectory will no longer influence slope/curve profile any more), which will greatly ease the problem solution. In addition, the input of space domain-based methods is the status of the preceding vehicle when it was at the ego vehicle's location and beyond (i.e. past status, rather than the current status). Since the input is past information and not time-sensitive, space domain-based methods are robust against packet loss and communication delay. Furthermore, space domain-based methods reduce formulation complexity. Taking eco-CACC as an example, when formulating in the time domain, the objective function has to include a mobility term on top of a fuel consumption term, otherwise, the optimal control would be standing still at all time (thus zero fuel consumption) [28]. This design not only increases the complexity of the optimization problem, but also casts potential doubt on the relative weighting between two terms. This does

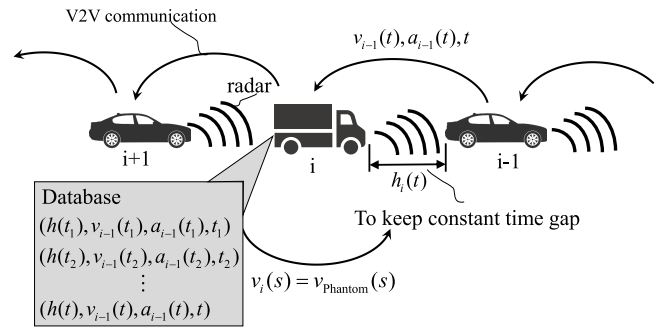


Fig. 1. CACC platoon.

not happen with space domain-based methods where only a fuel consumption term is needed. By default, the optimization objective becomes reducing fuel consumption over a given distance, rather than a time period. It is the textbook definition of fuel efficiency.

In summary, space-domain based methods simplify the incorporation of road curve/slope information into decision making and control process, thus enabling coordinated lateral/longitudinal control and facilitating eco-driving. In addition, past driving information of surrounding vehicles can be utilized in the space-domain design, which helps to improve robustness against communication loss. Therefore, this research focuses on developing a CACC system in the space domain. The main logic behind the system is to facilitate the host vehicle to learn from the preceding vehicle's past driving behavior, rather than the current one. The problem is formulated and solved by resorting to an optimal control method. The proposed system bears the following features:

- Enforcing a constant time gap between platoon members;
- Ensuring string stability with any time gap greater than the communication delay;
- Robust against packet loss and communication delay;
- Improved control precision by taking engine dynamics into account;
- Ensuring local stability and string stability.

The rest of this paper is organized as follows. Section II presents the control logic and problem formulation. Section III provides the solution method. Section IV gives the pseudocode for the implementation of the system. Section V proves the local stability and string stability. Section VI verifies the performance of the proposed system. Section VII discusses the pros and cons of the proposed system. Section VIII remarks the paper and introduces future plan.

II. CONTROL PROBLEM FORMULATION

In this section, the control logic and problem formulation of the proposed CACC system is presented.

A. Control Logic and Communication Topology

The control object is a fleet of CACC vehicles, as shown in figure 1. The communication topology of interest is predecessor-following. The ego vehicle collects the preceding

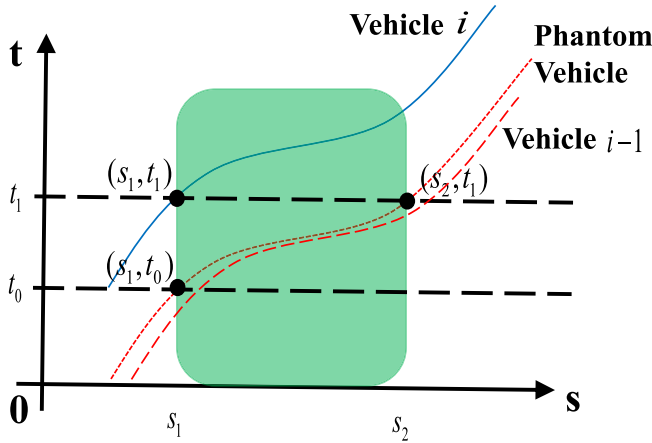


Fig. 2. Time-space diagram of vehicles' motion.

vehicle's status via V2V communication and obtains headway using radar. These collected data are then stored in a database. The data will be retrieved later and used as the control input. PF topology is adopted in this work. However, the proposed method can be easily adapted to accommodate other communication topologies such as predecessor-leader following (PLF). The problem is formulated in the space domain. The goal of the controller is to regulate a target time headway between platoon team members. Receding horizon control framework is adopted. In other words, at each update step, an optimal control problem is solved with only the first command in the solution being actuated.

B. Problem Formulation

To facilitate further discussion, definitions and notations are introduced here. The preceding vehicle is indexed as $i - 1$ and the ego vehicle indexed as i , as shown in figure 1 and figure 2. In this paper, a vehicle's location refers to the position of its front bumper. In figure 2, The dashed line is the trajectory of the preceding vehicle; the dotted line is the trajectory of the phantom vehicle, which is defined below; the solid line depicts the trajectory of the ego vehicle. At time instant t_1 , ego vehicle is at s_1 and phantom vehicle is at s_2 . Phantom vehicle passes s_1 at time instant t_0 .

Definition 1 (Phantom Vehicle): Phantom vehicle is an imaginary vehicle that keeps a constant distance away from the preceding vehicle. The bumper to bumper distance between the two vehicles is the summation of vehicle length and standstill distance. The phantom vehicle is introduced to simplify formulation. The standstill distance is a safety buffer to prepare the platoon for extreme conditions.

Definition 2 (Slowness): slowness [32] is the the change of time per unit distance, as a function of longitudinal position, denoted by w , $w(s) = dt/ds$.

Definition 3 (Moderation): moderation is the change of slowness per unit distance, as a function of longitudinal position, denoted by b , $b(s) = dw/ds$.

Definition 4 (Derk): derk is the change of moderation per unit distance, as a function of longitudinal position, $derk(s) = db/ds$.

TABLE I
VARIABLES IN THE SPACE DOMAIN AND THE TIME DOMAIN

Variables	Space Domain	Time Domain
Independent variable	s (longitudinal position)	t (time)
Dependent variable	t (time)	s (longitudinal position)
First-order derivative	w (slowness)	v (speed)
Second-order derivative	b (moderation)	a (acceleration)
Third-order derivative	derk	jerk
Relative dependent variable	g (time gap)	h (distance headway)

TABLE II
RELATIONS OF PHYSICAL QUANTITIES IN THE SPACE DOMAIN AND THE TIME DOMAIN

Variables	Space Domain ← Time Domain	Time Domain ← Space Domain
First-order derivative	$w = 1/v$	$v = 1/w$
Second-order derivative	$b = -a/v^3$	$a = -b/w^3$
Third-order derivative	$derk = 3a^2/v^5 - jerk/v^4$	$jerk = 3b^2/w^5 - derk/w^4$

For clarity of the variables defined, the variables in the space domain and its corresponding variables in the time domain are listed in TABLE I.

With the definitions of these variables, the relations between variables in the time domain and space domain could be derived, as listed in TABLE II. The proof of the relations is included in Appendix A.

The following details the formulation of the proposed CACC system. From this point on, variables v , a , $jerk$, h are functions of time, while \mathbf{x} , w , b , $derk$, g , L are functions of longitudinal position. We omit the argument in these variables when no ambiguity occurs.

1) *State and Control:* The state vector and control are as follows.

$$\mathbf{x} = [g_i - g^* \quad w_i - w_{\text{phantom}} \quad b_i]^T; \quad (1)$$

$$u = a_e. \quad (2)$$

where \mathbf{x} is the state vector; g_i is the time gap between the ego vehicle and the phantom vehicle; g^* is the desired time gap; w_i is the slowness of the ego vehicle; w_{phantom} is the slowness of the phantom vehicle; b_i is the moderation of ego vehicle; u is the control; a_e is the acceleration command put on the actuation system of the vehicle (also interpreted as the expected acceleration).

2) *Cost:* The objective is to find the control that minimizes the cost

$$\min_{\tilde{u}} J(s_1, \mathbf{x}(s_1) | \tilde{u}) = \int_{s=s_1}^{s_2} L(\mathbf{x}, u, s) ds + M(\mathbf{x}(s_2), s_2), \quad (3)$$

where \tilde{u} is the control sequence (with the control of each time instant combined together); J is the total cost; L is the running cost; M is the terminal cost.

In this study, the running cost is formulated in quadratic form and terminal cost as zero.

$$L(\mathbf{x}, u, s) = \frac{1}{2} \mathbf{x}^T \beta \mathbf{x}, \quad (4)$$

$$M(\mathbf{x}(s_2), s_2) = 0, \quad (5)$$

where β is diagonal matrix with β_1 , β_2 , and β_3 as diagonal entries. β_1 , β_2 , and β_3 are constant positive numbers. In this study, the terminal cost is set to zero since CACC is cruise control. This control aims to regulate the status of a vehicle during a journey. To put constraints on a vehicle's terminal state brings limited additional benefit while harming the controller's efficiency. This understanding is also shared by other studies on CACC optimal control [33].

By adopting this cost function form, it implies that the control rationale is to have the ego vehicle and phantom vehicle share the same speed at the same location. That is,

$$v_i(s) = v_{\text{phantom}}(s) \quad (6)$$

Proposition 1: If the ego vehicle and phantom vehicle keeping the same speed in segment $[s_1, s_2]$, then ego vehicle's time gap keep constant in this segment.

Proof: As the ego vehicle has the same motion as the phantom vehicle, the travel time of both vehicles covering the segment $[s_1, s](s \in [s_1, s_2])$ equal,

$$t_i(s) - t_i(s_1) = t_{\text{phantom}}(s) - t_{\text{phantom}}(s_1), \quad s \in [s_1, s_2], \quad (7)$$

where $t_{\text{phantom}}(s_1)$ and $t_{\text{phantom}}(s)$ are respectively the time instant when the phantom vehicle passes s_1 and s . The equation above directly leads to

$$t_i(s) - t_{\text{phantom}}(s) = t_i(s_1) - t_{\text{phantom}}(s_1), \quad s \in [s_1, s_2], \quad (8)$$

which means that the time gap is the same in $[s_1, s_2]$. ■

Notice that if ego vehicle is with desired time gap at s_1 , then the equation above is exactly the objective of the constant time gap CACC. The motion of the phantom vehicle in the segment of $[s_1, s_2]$ is the past driving information, which could be obtained by the ego vehicle and then stored in a database. The implication of the discussion above is that past information, which is rarely taken into consideration in previous works, is helpful to construct a constant time gap CACC system.

3) *Constraints:* The constraints are as follows.

$$-\frac{a_{\max}}{v^3} \leq b_i \leq -\frac{a_{\min}}{v^3}; \quad (9)$$

$$w_i \geq \frac{1}{v_{\max}}; \quad (10)$$

$$g_i > g_{\text{safe}}. \quad (11)$$

where a_{\min} and a_{\max} are respectively the minimum and maximum acceleration the ego vehicle can carry out; v_{\max} is the maximum speed; g_{safe} is a constant safe time gap. Among the three constraints, the first and second one are respectively transformed from the constraints on acceleration range and speed range in the time domain, while the last one is for safety consideration.

4) *Dynamics:* The first order inertia of the vehicle engine is taken into consideration. For convenience, the model of first-order inertia in the space domain is first given, based on which system dynamics of the proposed CACC is obtained.

Proposition 2: First order inertia in the space domain can be modelled as:

$$\text{der}k = \frac{3b^2}{w} + \frac{b_e - b}{\tau/w}, \quad (12)$$

where b_e is the moderation command (corresponding to a_e in the time domain); τ is time constant which represents engine dynamics.

Proof: first-order inertial [17] in the time domain is generally modelled as

$$\text{jer}k = \frac{a_e - a}{\tau}. \quad (13)$$

Based on the relations listed in table II, it could be derived that

$$\frac{3b^2}{w^5} - \frac{\text{der}k}{w^4} = \frac{1}{\tau} \left(\frac{-b_e}{w^3} - \frac{-b}{w^3} \right) \quad (14)$$

This equation above directly leads to proposition 2. ■

The first order derivatives of the three entries in state vector are

$$\frac{d(g_i - g^*)}{ds} = \frac{dg_i}{ds} = w_i - w_{\text{phantom}}; \quad (15)$$

$$\frac{d(w_i - w_{\text{phantom}})}{ds} = b_i - b_{\text{phantom}}; \quad (16)$$

$$\frac{db_i}{ds} = \text{der}k_i. \quad (17)$$

By denoting that

$$r = b_e + \frac{3b_i^2}{w_i^2} * \tau, \quad (18)$$

and approximating the dynamic of $\text{der}k$ as

$$\text{der}k_i = \dot{b}_i = \frac{r - b_i}{\tau/w_i} \approx \frac{r - b_i}{\tau/w_{\text{phantom}}}, \quad (19)$$

the dynamic function then can be formulated as

$$\mathbf{f} = \mathbf{R} \approx \mathbf{A}\mathbf{x} + \mathbf{B}\mathbf{r} + \mathbf{C}b_{\text{phantom}}, \quad (20)$$

with

$$\mathbf{A} = \begin{bmatrix} 0 & 1 & 0 \\ 0 & 0 & 1 \\ 0 & 0 & -w_{\text{phantom}}/\tau \end{bmatrix}; \quad (21)$$

$$\mathbf{B} = \begin{bmatrix} 0 \\ 0 \\ w_{\text{phantom}}/\tau \end{bmatrix}; \quad (22)$$

$$\mathbf{C} = \begin{bmatrix} 0 \\ -1 \\ 0 \end{bmatrix}, \quad (23)$$

where b_{phantom} is the moderation of phantom vehicle.

Equation (19) is based on the observation that the control objective is to draw the ego vehicle's speed to that of the phantom vehicle, as shown in section II-A. As slowness is the reciprocal of speed (see table II), the two vehicles' slowness at

the same location is basically the same, $w_i = w_{b_{\text{phantom}}}$. With this approximation, the system then can be regarded as a linear position-invariant system (similar to linear time-invariant system in the time domain), as the matrices \mathbf{A} , \mathbf{B} , and \mathbf{C} are all independent with \mathbf{x} and r .

Algorithm 1 Solution for the Optimal Control Problem

Input: initial state $\mathbf{x}(s_1)$, preceding vehicle's trajectory $\Theta_{s_1}, \Theta_1, \dots, \Theta_{s_2}$, cost preference β , time constant τ ▷ See figure 3 for explanation of preceding vehicle's trajectory

Output: control $u(k)$ and state $\mathbf{x}(k)$ of each control step

Discretization

- 1: set total control steps $W = \text{count}(\Theta_{s_1}, \Theta_1, \dots, \Theta_{s_2}) - 1$
- 2: Compute the discrete dynamics $\mathbf{A}_k = \mathbf{I} + \mathbf{A} \Delta s_k$, $\mathbf{B}_k = \mathbf{B} \Delta s_k$, $\mathbf{C}_k = \mathbf{C} b_k \Delta s_k$, $\beta_k = \beta \Delta s_k$ ▷ See figure 3 for definition of Δs_k

Initialization

- 3: Set $\mathbf{Q}_W = \beta_k$, $\mathbf{D}_W = \mathbf{0}$, and $\mathbf{E}_W = \mathbf{0}$
- 4: Set $\tilde{\mathbf{Q}}_W = \mathbf{Q}_W$, $\tilde{\mathbf{D}}_W = \mathbf{D}_W$, and $\tilde{\mathbf{E}}_W = \mathbf{E}_W$

Backward compute concomitant matrices

- 5: **for** k in $\{W - 1, \dots, 1\}$ **do**
- 6: $\mathbf{P}_k := (\mathbf{B}_k^T \tilde{\mathbf{Q}}_{k+1} \mathbf{B}_k)^{-1}$
- 7: $\mathbf{G}_k := -\mathbf{P}_k \mathbf{B}_k^T \tilde{\mathbf{Q}}_{k+1} \mathbf{A}_k$
- 8: $\mathbf{H}_k := -\mathbf{P}_k \mathbf{B}_k^T (\tilde{\mathbf{Q}}_{k+1} \mathbf{C}_k + \tilde{\mathbf{D}}_{k+1})$
- 9: $\mathbf{S}_k := \mathbf{A}_k + \mathbf{B}_k \mathbf{G}_k$
- 10: $\mathbf{T}_k := \mathbf{B}_k \mathbf{H}_k + \mathbf{C}_k$
- 11: $\tilde{\mathbf{Q}}_k := \mathbf{S}_k^T \tilde{\mathbf{Q}}_{k+1} \mathbf{S}_k + \beta_k$
- 12: $\tilde{\mathbf{D}}_k := \mathbf{S}_k^T \tilde{\mathbf{Q}}_{k+1} \mathbf{T}_k + \mathbf{S}_k^T \tilde{\mathbf{D}}_{k+1}$
- 13: $\tilde{\mathbf{E}}_k := \frac{1}{2} \mathbf{T}_k^T \tilde{\mathbf{Q}}_{k+1} \mathbf{T}_k + \mathbf{T}_k^T \mathbf{D}_{k+1} + \tilde{\mathbf{E}}_{k+1}$
- 14: **end for**

Forward compute control and state

- 15: **for** k in $\{0, \dots, W - 1\}$ **do**
 - 16: compute r : $r(k) = \mathbf{G}_k \mathbf{x}(k) + \mathbf{H}_k$
 - 17: compute the next state: $\mathbf{x}(k+1) = \mathbf{S}_k \mathbf{x}(k) + \mathbf{T}_k$
 - 18: **if** the any constraint on the next state activates **then**
 - 19: set the acceleration at the next state as the maximum feasible acceleration a_{feasible}
 - 20: set the next acceleration $a_i(k+1) = \min[\max(a_{\min}, a_{\text{feasible}}), a_{\max}]$
 - 21: compute the control ▷ See equation (24)
 - 22: compute $r(k)$ ▷ See equation (18)
 - 23: $\mathbf{x}(k+1) = \mathbf{A}_k \mathbf{x}(k) + \mathbf{B}_k r(k) + \mathbf{C}_k$
 - 24: **else**
 - 25: compute the control ▷ See equation (25)
 - 26: **end if**
 - 27: **end for**
-

III. SOLUTION

This section gives the solution to the optimal control problem formulated in section II-B. This solution, as shown in algorithm 1, was previously proposed by this research team [34]. The idea is inspired by dynamic programming and proved to be of local quadratic convergence. The algorithm first discretizes the proposed continuous problem, with total control steps equal to the number of data collected. After that, the costs of each time instant are accumulated backward by

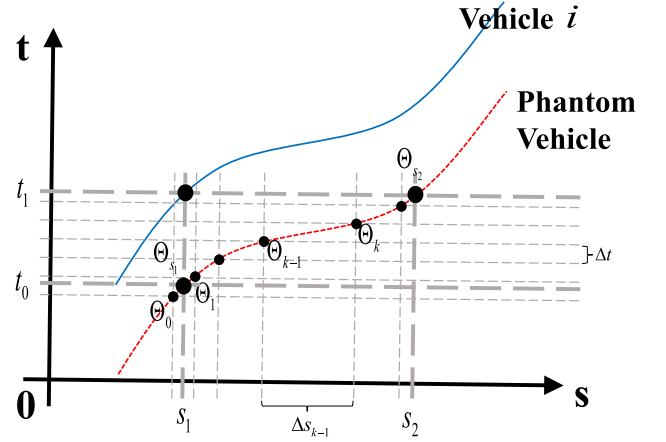


Fig. 3. Data Collection.

computing concomitant matrices. At last the optimal control and the optimal state are forward computed.

The constraints on slowness and time gap are explicitly handled by rectifying the acceleration to be the maximum feasible acceleration. Then the constraints on acceleration are handled by adopting minimum acceleration or maximum acceleration. With any constraints activated, the control is rectified to be

$$u(k) = \frac{\tau}{w_i \Delta s_k} [a_i(k+1) - a_i(k)] + a_i(k), \quad (24)$$

where k is the control step index. The equation above guarantees that the acceleration of the next state will be feasible.

With no constraints activated, the control law is

$$u(k) = - \left(r(k) - \frac{3b_i^2}{w_i^2} \times \tau \right) / w_i^3, \quad (25)$$

which is derived directly from equation (18)

IV. PSEUDO CODE

The pseudo code of the proposed control method is given in pseudocode 1. The pseudo code consists of four parts: data collection, trajectory planning, database management, and actuation.

A. Data Collection

The data collected are in the time domain (h, v_{i-1}, a_{i-1}) , as it is the most prevailing way to gather data. Data are retrieved every Δt seconds, as shown in figure 3. This mechanism can be easily realized by adding a timer to the system. The collected data is first stored into the ego vehicle's database and then converted into the variables in the space domain. Preceding vehicle's motion at s_1 and s_2 are then interpolated. It needs to be noted that when converting the variables from the time domain into the space domain, the object of interest also changes from the preceding vehicle to the phantom vehicle.

Even though, in the current setting, the solution method shall use input data in the time domain, the solution could be

Pseudocode 1 Solution for the Proposed CACC

Input: desired time gap g^* , cost preference β , vehicle length L , standstill distance $s_{\text{standstill}}$

Output: control a_e

1: **repeat**

Data collection

2: collect preceding vehicle's motion at each time instant $(h_i, v_{i-1}, a_{i-1}, t)$

3: store the collected information into database

4: retrieve the data $\Theta_0, \Theta_1, \dots, \Theta_{k-1}, \Theta_k, \dots$ from the database \triangleright See figure 3

5: transform the retrieved data into the space domain (w_{i-1}, b_{i-1}, s) \triangleright See section II-B

6: compute the phantom vehicle's trajectory $(w_{\text{phantom}}, b_{\text{phantom}}, s)$ by shifting the preceding vehicle's trajectory upstream by $L + s_{\text{standstill}}$

7: Interpolate the phantom vehicle's motion at s_1 and s_2 , that is $\Theta_{s_1} = (w_{\text{phantom}}, b_{\text{phantom}}, s_1)$ and $\Theta_{s_2} = (w_{\text{phantom}}, b_{\text{phantom}}, s_2)$

Trajectory planning

8: set $g_i(s_1) = \sum_{s=s_1}^{s_2} w_{\text{phantom}}(s) \times \Delta s_k$

9: set initial state $\mathbf{x}(s_1) = [g_i(s_1) - g^* \ w_i(s_1) - w_{\text{phantom}}(s_1) \ b_i(s_1)]^T$

10: planning the trajectory \triangleright See algorithm 1

Database management

11: **for all** entries $(h_i, v_{i-1}, a_{i-1}, t)$ in database **do**

12: **if** time stamp of this entry and the next entry are both less than t_0 **then**

13: delete this entry

14: **end if**

15: **end for**

Actuation

16: ego vehicle actuates the first of the computed control

17: **until** End

easily modified to handle with the case of data collection in the space domain by omitting the step 5 in the solution. Using input data in the time domain is actually an upgrade, as it is more practical and reliable to collect data in the time domain.

B. Trajectory Planning

The longitudinal trajectory between s_1 and s_2 are computed by using the method proposed in this paper. This is the core of the proposed method.

C. Database Management

As the trajectory planning process involves preceding vehicle's past driving information, a database is required.

After trajectory being planned, the data collected before Θ_0 will be removed from the database. This guarantees that the memory required is reduced to the minimum. As outdated data is periodically cleared, the stored data is quite small compared with the capability of today's regular computers. For instance, if data are collected 10 times a second, with desired headway

being 2 seconds, there will be only around 20 entries in the database.

D. Actuation

The acceleration command, which is given by the trajectory planning algorithm (see Algorithm 1), then can be actuated by the ego vehicle's actuation system [15], [17], [18].

V. STABILITY ANALYSIS

Local stability and string stability, two primary concerns when designing CACC systems, are discussed in this section. Both the local and string stability of the proposed CACC system are analyzed. Please be aware that the proof provided in this section is only valid when the constraints are not activated. The proposed controller is only proven to be local-stable and string-stable under regular cruising conditions when no constraint is activated. Proofs of the proposed controller's stability under constraints will be considered in the following study.

We first prove Lemma 1, which gives the linear relationship between the state, control, and co-state [35]. Based on the linear relationship given in Lemma 1, the local stability proof and string stability proof are given.

Lemma 1: Writing the related matrices as block matrices (those with subscript upper are of two rows and those with subscript down are of one row) as

$$\mathbf{A} = \begin{bmatrix} \mathbf{A}_{\text{upper}} & \mathbf{A}_{\text{ud}} \\ \mathbf{0} & \mathbf{A}_{\text{down}} \end{bmatrix}, \quad (26)$$

$$\mathbf{B} = \begin{bmatrix} \mathbf{0} \\ \mathbf{B}_{\text{down}} \end{bmatrix}, \quad (27)$$

$$\mathbf{C} = \begin{bmatrix} \mathbf{C}_{\text{upper}} \\ \mathbf{0} \end{bmatrix}, \quad (28)$$

$$\mathbf{x} = \begin{bmatrix} \mathbf{x}_{\text{upper}} \\ \mathbf{x}_{\text{down}} \end{bmatrix}, \quad (29)$$

$$\lambda = \begin{bmatrix} \lambda_{\text{upper}} \\ \lambda_{\text{down}} \end{bmatrix}, \quad (30)$$

$$\beta = \begin{bmatrix} \beta_{\text{upper}} & \mathbf{0} \\ \mathbf{0} & \beta_{\text{down}} \end{bmatrix}. \quad (31)$$

The state, control, and co-state then have the following relationship.

$$\dot{\mathbf{x}}_{\text{upper}} = \mathbf{A}_{\text{upper}}\mathbf{x}_{\text{upper}} + \mathbf{A}_{\text{ud}}\mathbf{x}_{\text{down}} + \mathbf{C}_{\text{upper}}b_{\text{phantom}}; \quad (32)$$

$$-\dot{\lambda}_{\text{upper}} = \beta_{\text{upper}}\mathbf{x}_{\text{upper}} + \mathbf{A}_{\text{upper}}^T\lambda_{\text{upper}}; \quad (33)$$

$$\beta_{\text{down}}\mathbf{x}_{\text{down}} + \mathbf{A}_{\text{ud}}^T\lambda_{\text{upper}} = \mathbf{0}. \quad (34)$$

The proof is included in appendix B. \blacksquare

A. Local Stability

Theorem 1 (Local Stability of the CACC in the Space Domain): The proposed CACC is local-stable if $\beta_1 > 0$, $\beta_2 > 0$, and $\beta_3 > 0$.

TABLE III
BENEFIT OF THE SPACE DOMAIN-BASED CACC

	V.S. baseline CACC				V.S. \mathcal{H}_∞ synthesis-based CACC			
	Fuel	Emission	ST	OAR	Fuel	Emission	ST	OAR
(0%, 0ms)	0.35%	0.48%	20.14%	-5.32%	1.81%	1.53%	11.03%	-3.72%
(5%, 100ms)	4.88%	3.78%	20.89%	2.02%	5.65%	4.32%	11.86%	1.34%
(20%, 500ms)	16.11%	12.40%	25.90%	23.82%	14.60%	11.20%	17.45%	21.60%

VI. VERIFICATION

The proposed CACC system is evaluated against a \mathcal{H}_∞ synthesis-based controller [18], [31] and a prevailing linear feedback controller [17]. The goal is to evaluate the proposed controller in the following aspects: stability, performance on fuel consumption and emission, and robustness against communication failure.

A. Experiment Design

Two scenarios are designed to respectively verify the local stability and string stability. Local stability scenario initiates with a non-stable state, with preceding vehicle runs with constant speed in the simulation horizon. In string stability scenario, preceding vehicle's longitudinal motion oscillates periodically. A homogeneous fleet is assumed, similar to [17], [18], [31]. For each scenario, the following three controllers are tested:

Proposed CACC: In this case, the proposed CACC controls the car-following behavior of the ego vehicle.

\mathcal{H}_∞ synthesis-based CACC: In this case, both the feedback and feedforward controllers are designed by adopting the \mathcal{H}_∞ synthesis approach introduced in [18], [31].

Baseline CACC: In the baseline scenarios, feedback-based CACC [17] is adopted.

To consider stochasticity, for each scenario, ten simulation runs with different random seeds are carried out. More random seeds are run if sample size check does not pass after ten runs. Result values from different runs are averaged to acquire the final results.

B. Sensitivity Analysis

Sensitivity analysis is conducted in terms of communication failure. Packet loss and communication delay are considered. Tested levels of packet loss rate and communication delay are: (0%, 0 ms), (5%, 100 ms), and (20%, 500 ms).

C. Measurement of Effectiveness

The adopted Measurements of effectiveness (MOE) are fuel consumption, CO₂ emission, stabilization time (ST), and Oscillation Absorbing Rate (OAS). Fuel consumption and emission are computed using VT-micro model [41], [42]. Stabilizing time is measured as the time elapsed until acceleration falls short of a threshold (which is 0.15 m/s² in this paper) in local stability scenario. Oscillation absorbing rate is defined as

$$OAS = \frac{a_f^{\max} - a^{\max}}{a_f^{\max}}, \quad (51)$$

where *OAS* is oscillation absorbing rate, a_f^{\max} and a^{\max} are respectively the maximal acceleration/deceleration of preceding vehicle and ego vehicle in the string stability scenario.

D. Control Settings

Parameters for the proposed CACC, \mathcal{H}_∞ synthesis-based CACC, and baseline CACC are carefully tuned for a fair comparison. Vehicle length, standstill distance, and desired time gap are the same to guarantee the same mobility. Communication frequency and control frequency are also the same to guarantee the same workload for the communication system and control system. Furthermore, the cost preference of the proposed CACC is tuned to produce basically the same fuel consumption and emission as the \mathcal{H}_∞ synthesis-based CACC and the baseline CACC when communication quality is good, as shown in table III.

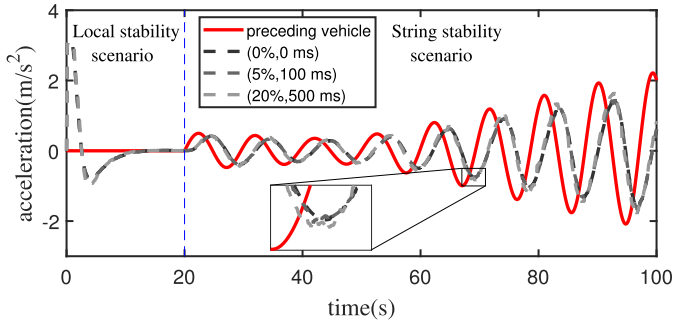
The following setting are made for the proposed controller.

- **simulation setting:** simulation horizon for local stability scenario: 20 s; simulation horizon for string stability scenario: 280 s; communication frequency: 10 Hz; control frequency: 20 Hz.
- **vehicle setting:** vehicle length $L = 5$ m; time constant $\tau = 1.0$ s.
- **control parameters:** standstill distance $s_{\text{standstill}} = 2$ m; desired time gap $g^* = 1.5$ s; cost preference $\beta = \text{diag}(1, 30^2, 30^4)$; acceleration range: $[-5, 3]$ m/s².
- **preceding vehicle's motion:** preceding vehicle runs with stable speed in the local stability scenario and periodically accelerates and decelerates in the string stability scenario with angular speed 0.21π , 0.22π , 0.23π . The amplitude of the three elements are 1.0 m/s², -1.0 m/s², 0.5 m/s²;
- **initial state:** in local stability scenario, initial headway: 45 m; initial speed of preceding vehicle: 20 m/s; initial speed of ego vehicle: 18 m/s; in string stability scenario, initial state is stable state.

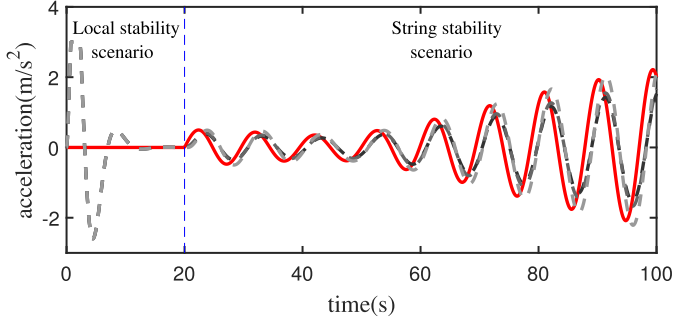
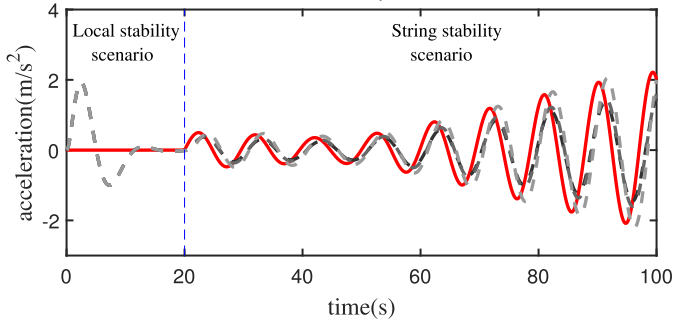
The control parameters for the baseline CACC is: $k_p = 0.2$, $k_{d1} = 0.7$, $k_{d2} = 0$, as same as the ones in [17]. The control parameters for the \mathcal{H}_∞ synthesis-based controller is directly derived by the \mathcal{H}_∞ optimization method.

E. Simulation Result

The proposed CACC system generally outperforms the \mathcal{H}_∞ synthesis-based CACC and the baseline CACC respectively with benefits of up to 21.60% and 25.90%. The benefits of the proposed CACC is shown in table III. All benefits in table III are averaged results over multiple random seeds runs, with positive numbers showing improvement and negative ones showing deterioration.



(a) Acceleration of the the proposed CACC

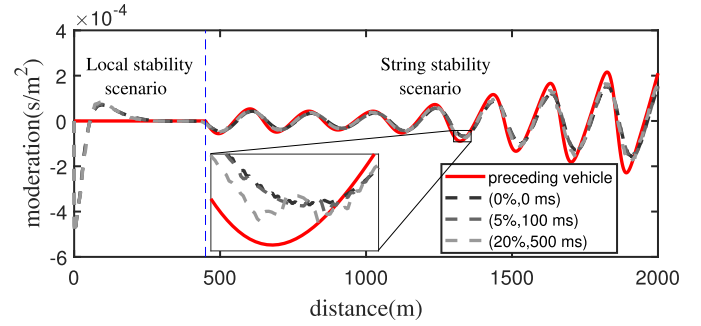
(b) Acceleration of the \mathcal{H}_∞ synthesis-based CACC

(c) Acceleration of the baseline CACC

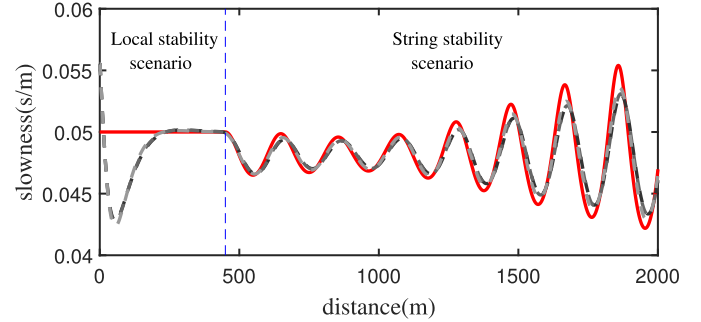
Fig. 5. Acceleration Profile. Note that all the three subfigures share the same legend.

Compare with the \mathcal{H}_∞ synthesis-based CACC and the baseline CACC, the proposed CACC helps to reduce fuel consumption and emission. The benefit of fuel consumption reduction ranges from 0.35% to 16.11%, while the benefit of CO₂ emission ranges from 0.48% to 12.40%. Furthermore, the proposed CACC stabilizes the ego vehicle faster, with ST benefit ranging from 11.03% to 25.90%. The benefit of OAR is from -5.32% to 23.82%, which demonstrates a positive effect on reducing downstream oscillation. It should be noted that the tested level of (0%, 0ms) is employed to tune controller parameters. In order to facilitate a fair apple-to-apple comparison, it was the goal to make sure the three tested controllers perform similarly at least one level. However, it is not possible to have all measurements having a benefit of zero. With the other benefits being close to zero, OAR equals to -5.32% and -3.72% is the closest one could get. Therefore, the negative percentages in the first row of TABLE III is a result of the experiment setting. It does not indicate an adverse effect.

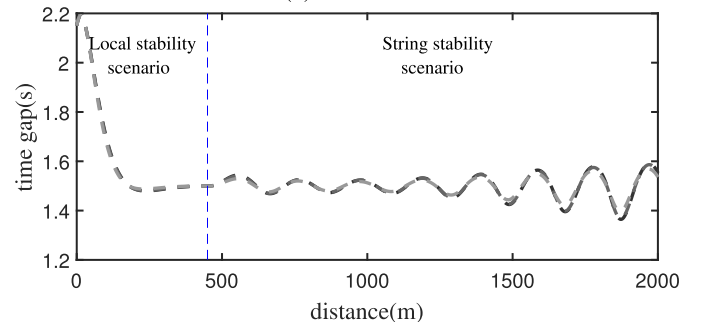
The trajectory of the fleet under the control of the three controllers tested are shown in figure 5 and 6. To save space,



(a) Moderation



(b) Slowness



(c) Time gap

Fig. 6. Simulation result. desired time gap $g^* = 1.5$ s; cost preference $\beta = \text{diag}(1, 30^2, 30^4)$; initial headway: 45 m; initial speed of preceding vehicle: 20 m/s; initial speed of ego vehicle: 18 m/s. Note that all the three subfigures share the same legend.

the local stability and string stability scenarios are shown in the same figure. The figures demonstrate that the proposed controller is much more robust against communication failure. Package loss and communication delay both have minimal influence on the performance of the proposed CACC system. While feedback-based CACC fails string stability as communication delay increases. Admittedly, poor communication quality does influence the smoothness of the proposed control as well. As shown in figure 5a and 6a, there are some “sawtooth” in follower’s acceleration and moderation, which will hamper the driving comfort. But if compared to the baseline, it is still a pretty good performance.

Computation speed of the proposed solution is quite fast. The average computation time on a regular laptop (operating system: Windows 10, workbench: Matlab R2017b, CPU: Intel i7-6700HQ) is 1.26 ms. The computation speed indicates the proposed controller’s potential to be applied in real-time.

VII. DISCUSSION

In this section, the advantages and disadvantages of the proposed CACC system are discussed in detail.

One of the main benefits of the space domain-based CACC is strong robustness against packet loss and communication delay, which are two of the main factors influencing the CACC system's performance. This is originated from the fact that the proposed system mainly utilizes past data, instead of current data. Lost packages have no significant effect as the missing information could be filled by the neighboring packages. This is based on the fact that the vehicle's motion changes relatively slowly, and the missing information about the lost package is similar to that of the data nearby. Communication delay, on the other hand, which influences only on the receiving of the last few packages, could be regarded as a special case of packet loss, thus has a minimal influence as well.

Another advantage is that, unlike the conventional feedback-based CACC systems where a minimum headway is required for string stability insurance [15], [17], string stability of the proposed CACC control is guaranteed with any positive headway which is greater than the communication delay. This means smaller headway is technically feasible with the proposed controller. Since smaller headway equals to higher traffic throughput, the proposed controller is also beneficial to traffic mobility.

The proposed controller performs well to keep constant time gap for uninterrupted traffic flow. However, it will run into errors in the situation of stop-and-go traffic. When speed approaches zero, slowness, which is the reciprocal of speed, would tend to be infinite. This makes it hard to find an efficient numerical solution.

VIII. CONCLUSION

In this research, a new Cooperative Adaptive Cruise Control (CACC) controller in the space domain is proposed, with all the variables as functions of longitudinal position, instead of time. This CACC is based on optimal control. The proposed controller is able to enforce a target time headway between platoon members. By formulating the CACC in the space domain, instead of time domain, its robustness against communication failure is greatly improved and thus minimum safety headway buffer is reduced which leads to better mobility. In addition, third-order vehicle dynamics are modeled into the proposed control in order to improve control precision when implemented in the field. Local stability and string stability are theoretically proven. The proposed controller is evaluated in a MATLAB simulation against two state-of-the-art controllers. Results reveal that the proposed CACC system outperforms the state-of-the-art controllers. Computation speed of the proposed method is 1.26 ms on a regular laptop (operating system: Windows 10, workbench: Matlab R2017b, CPU: Intel i7-6700HQ). The computation speed indicates the proposed controller's potential to be applied in real-time. The features of the proposed controller are highlighted as follows:

- Formulated in the space domain and enforcing a constant time gap between platoon members;
- Ensuring string stability with any time gap greater than the communication delay;

- Robust against packet loss and communication delay;
- Improved control precision by taking engine dynamics into account;
- Improving local stability from 11.03% to 25.90%, and string stability by up to 23.82%;
- Reducing fuel consumption from 0.35% to 16.11% and reducing CO₂ emission from 0.48% to 12.40%.

Due to the nature that slope/curve information is more closely related to position, instead of time, the space domain-based methods can incorporate these kinds of road information more easily. For this reason, apart from the constant time gap CACC, the control method in the space domain could also be applied to other vehicle control problems, such as eco-driving and vehicle lateral control. The application of the space domain-based methods to these two kinds of problems will be included in future work. Furthermore, poor communication quality does influence the smoothness of control of the proposed CACC system. Improving the control smoothness will also be included in future work.

APPENDIX A

RELATIONS OF VARIABLES IN THE TIME DOMAIN AND THE SPACE DOMAIN

The relationship between v and w is as follows.

$$w = dt/ds = 1/(ds/dt) = 1/v, \quad (\text{A.1})$$

$$v = ds/dt = 1/(dt/ds) = 1/w. \quad (\text{A.2})$$

Based on the above two equations, it could be derived that

$$b = \frac{dw}{ds} = \frac{d(1/v)}{ds} = -\frac{1}{v^2} \frac{dv}{ds} = -\frac{1}{v^2} \frac{dv}{dt} \frac{dt}{ds} = -\frac{a}{v^3}, \quad (\text{A.3})$$

$$a = \frac{dv}{dt} = \frac{d(1/w)}{dt} = -\frac{1}{w^2} \frac{dw}{dt} = -\frac{1}{w^2} \frac{dw}{ds} \frac{ds}{dt} = -\frac{b}{w^3}. \quad (\text{A.4})$$

It then could be derived that

$$\begin{aligned} \text{derk} &= \frac{db}{ds} = \frac{d(-a/v^3)}{ds} = \left(\frac{3a}{v^4} \frac{dv}{dt} - \frac{1}{v^3} \frac{da}{dt} \right) \frac{dt}{ds} \\ &= \left(\frac{3a}{v^4} a - \frac{1}{v^3} \text{jerk} \right) \frac{1}{v} \\ &= \frac{3a^2}{v^5} - \frac{\text{jerk}}{v^4}, \end{aligned} \quad (\text{A.5})$$

$$\begin{aligned} \text{jerk} &= \frac{da}{dt} = \frac{d(-b/w^3)}{dt} = \left(\frac{3b}{w^4} \frac{dw}{ds} - \frac{1}{w^3} \frac{db}{ds} \right) \frac{ds}{dt} \\ &= \left(\frac{3b}{w^4} b - \frac{1}{w^3} \text{derk} \right) \frac{1}{w} \\ &= \frac{3b^2}{w^5} - \frac{\text{derk}}{w^4}. \end{aligned} \quad (\text{A.6})$$

APPENDIX B

PROOF OF LEMMA 1

Substituting the block matrices (26) - (31) in dynamic function (20), it could be derived that

$$\begin{aligned} \begin{bmatrix} \dot{\mathbf{x}}_{\text{upper}} \\ \dot{\mathbf{x}}_{\text{down}} \end{bmatrix} &= \begin{bmatrix} \mathbf{A}_{\text{upper}} & \mathbf{A}_{\text{ud}} \\ \mathbf{0} & \mathbf{A}_{\text{down}} \end{bmatrix} \begin{bmatrix} \mathbf{x}_{\text{upper}} \\ \mathbf{x}_{\text{down}} \end{bmatrix} \\ &+ \begin{bmatrix} \mathbf{0} \\ \mathbf{B}_{\text{down}} \end{bmatrix} r + \begin{bmatrix} \mathbf{C}_{\text{upper}} \\ \mathbf{0} \end{bmatrix} b_{\text{phantom}}, \end{aligned} \quad (\text{B.1})$$

which gives

$$\dot{\mathbf{x}}_{\text{upper}} = \mathbf{A}_{\text{upper}}\mathbf{x}_{\text{upper}} + \mathbf{A}_{\text{ud}}\mathbf{x}_{\text{down}} + \mathbf{C}_{\text{upper}}b_{\text{phantom}}. \quad (\text{B.2})$$

Pontryagin's minimum principle (PMP) [35] gives the following relationship between state, co-state (λ), and control.

$$-\dot{\lambda} = \beta\mathbf{x} + \mathbf{A}^T\lambda, \quad (\text{B.3})$$

$$\mathbf{B}^T\lambda = \mathbf{0}. \quad (\text{B.4})$$

Substituting the block matrices (26) - (31) in Eq. (B.3), it gives

$$-\begin{bmatrix} \dot{\lambda}_{\text{upper}} \\ \dot{\lambda}_{\text{down}} \end{bmatrix} = \begin{bmatrix} \beta_{\text{upper}} & \mathbf{0} \\ \mathbf{0} & \beta_{\text{down}} \end{bmatrix} \begin{bmatrix} \mathbf{x}_{\text{upper}} \\ \mathbf{x}_{\text{down}} \end{bmatrix} + \begin{bmatrix} \mathbf{A}_{\text{upper}} & \mathbf{A}_{\text{ud}} \\ \mathbf{0} & \mathbf{A}_{\text{down}} \end{bmatrix}^T \begin{bmatrix} \lambda_{\text{upper}} \\ \lambda_{\text{down}} \end{bmatrix}. \quad (\text{B.5})$$

Then the following two equations are obtained

$$-\dot{\lambda}_{\text{upper}} = \beta_{\text{upper}}\mathbf{x}_{\text{upper}} + \mathbf{A}_{\text{upper}}^T\lambda_{\text{upper}}, \quad (\text{B.6})$$

$$-\dot{\lambda}_{\text{down}} = \beta_{\text{down}}\mathbf{x}_{\text{down}} + \mathbf{A}_{\text{ud}}^T\lambda_{\text{upper}} + \mathbf{A}_{\text{down}}^T\lambda_{\text{down}}. \quad (\text{B.7})$$

Substituting the block matrices (26) - (31) in Eq. (B.4), it gives

$$\begin{bmatrix} \mathbf{0} \\ \mathbf{B}_{\text{down}} \end{bmatrix}^T \begin{bmatrix} \lambda_{\text{upper}} \\ \lambda_{\text{down}} \end{bmatrix} = \mathbf{0}, \quad (\text{B.8})$$

which indicates

$$\mathbf{B}_{\text{down}}^T\lambda_{\text{down}} = \mathbf{0}. \quad (\text{B.9})$$

Combining Eq. (B.7) and (B.9), it derives that

$$\beta_{\text{down}}\mathbf{x}_{\text{down}} + \mathbf{A}_{\text{ud}}^T\lambda_{\text{upper}} = \mathbf{0}. \quad (\text{B.10})$$

Equation (B.2), (B.6), (B.10) are exactly the relationships that need to be proved.

REFERENCES

- [1] K. C. Dey *et al.*, "A review of communication, driver characteristics, and controls aspects of cooperative adaptive cruise control (CACC)," *IEEE Trans. Intell. Transp. Syst.*, vol. 17, no. 2, pp. 491–509, Feb. 2016.
- [2] V. Milanés, S. E. Shladover, J. Spring, C. Nowakowski, H. Kawazoe, and M. Nakamura, "Cooperative adaptive cruise control in real traffic situations," *IEEE Trans. Intell. Transp. Syst.*, vol. 15, no. 1, pp. 296–305, Feb. 2014.
- [3] G. Orosz, "Connected cruise control: Modelling, delay effects, and nonlinear behaviour," *Vehicle Syst. Dyn.*, vol. 54, no. 8, pp. 1147–1176, Aug. 2016.
- [4] Y. Bian, Y. Zheng, W. Ren, S. E. Li, J. Wang, and K. Li, "Reducing time headway for platooning of connected vehicles via V2V communication," *Transp. Res. C, Emerg. Technol.*, vol. 102, pp. 87–105, May 2019.
- [5] W. B. Qin and G. Orosz, "Experimental validation of string stability for connected vehicles subject to information delay," *IEEE Trans. Control Syst. Technol.*, Apr. 11, 2019. [Online]. Available: <https://ieeexplore.ieee.org/abstract/document/8685673>, doi: 10.1109/TCST.2019.2900609.
- [6] D. Lang, R. Schmied, and L. Del Re, "Prediction of preceding driver behavior for fuel efficient cooperative adaptive cruise control," *SAE Int. J. Engines*, vol. 7, no. 1, pp. 14–20, 2014.
- [7] S. E. Shladover, D. Su, and X.-Y. Lu, "Impacts of cooperative adaptive cruise control on freeway traffic flow," *Transp. Res. Rec., J. Transp. Res. Board*, vol. 2324, no. 1, pp. 63–70, Jan. 2012.
- [8] B. van Arem, C. J. G. van Driel, and R. Visser, "The impact of cooperative adaptive cruise control on traffic-flow characteristics," *IEEE Trans. Intell. Transp. Syst.*, vol. 7, no. 4, pp. 429–436, Dec. 2006.
- [9] C. Yu, Y. Feng, H. X. Liu, W. Ma, and X. Yang, "Integrated optimization of traffic signals and vehicle trajectories at isolated urban intersections," *Transp. Res. B, Methodol.*, vol. 112, pp. 89–112, Jun. 2018.
- [10] S. E. Shladover, C. Nowakowski, X. Lu, and R. Hoogendoorn, "Using cooperative adaptive cruise control (CACC) to form high-performance vehicle streams," PATH, San Jose, CA, USA, Tech. Rep., 2014. [Online]. Available: <https://escholarship.org/uc/item/3m89p611>
- [11] C. Nowakowski, S. E. Shladover, X. Lu, D. Thompson, and A. Kailas, "Cooperative adaptive cruise control (CACC) for truck platooning: Operational concept alternatives," PATH, San Jose, CA, USA, Tech. Rep., 2015. [Online]. Available: <https://escholarship.org/uc/item/7jf9n5wm#main>
- [12] Y. Zheng, S. E. Li, K. Li, and W. Ren, "Platooning of connected vehicles with undirected topologies: Robustness analysis and distributed H-infinity controller synthesis," *IEEE Trans. Intell. Transp. Syst.*, vol. 19, no. 5, pp. 1353–1364, May 2018.
- [13] Y. Li, W. Chen, S. Peeta, and Y. Wang, "Platoon control of connected multi-vehicle systems under V2X communications: Design and experiments," *IEEE Trans. Intell. Transp. Syst.*, early access, Apr. 11, 2019. [Online]. Available: <https://ieeexplore.ieee.org/abstract/document/8686052>, doi: 10.1109/TITS.2019.2905039.
- [14] Y. Zheng, S. E. Li, J. Wang, L. Y. Wang, and K. Li, "Influence of information flow topology on closed-loop stability of vehicle platoon with rigid formation," in *Proc. 17th Int. IEEE Conf. Intell. Transp. Syst. (ITSC)*, Oct. 2014, pp. 2094–2100.
- [15] G. J. L. Naus, R. P. A. Vugts, J. Ploeg, M. J. G. van de Molengraft, and M. Steinbuch, "String-stable CACC design and experimental validation: A frequency-domain approach," *IEEE Trans. Veh. Technol.*, vol. 59, no. 9, pp. 4268–4279, Nov. 2010.
- [16] D. Hajdu, J. I. Ge, T. Insperger, and G. Orosz, "Robust design of connected cruise control among human-driven vehicles," *IEEE Trans. Intell. Transp. Syst.*, vol. 21, no. 2, pp. 749–761, Feb. 2020, doi: 10.1109/tits.2019.2897149.
- [17] J. Ploeg, B. T. M. Scheepers, E. van Nunen, N. van de Wouw, and H. Nijmeijer, "Design and experimental evaluation of cooperative adaptive cruise control," in *Proc. 14th Int. IEEE Conf. Intell. Transp. Syst. (ITSC)*, Oct. 2011, pp. 260–265.
- [18] J. Ploeg, D. P. Shukla, N. van de Wouw, and H. Nijmeijer, "Controller synthesis for string stability of vehicle platoons," *IEEE Trans. Intell. Transp. Syst.*, vol. 15, no. 2, pp. 854–865, Apr. 2014.
- [19] M. Wang, W. Daamen, S. P. Hoogendoorn, and B. van Arem, "Rolling horizon control framework for driver assistance systems. Part I: Mathematical formulation and non-cooperative systems," *Transp. Res. C, Emerg. Technol.*, vol. 40, pp. 271–289, Mar. 2014.
- [20] M. Wang, W. Daamen, S. P. Hoogendoorn, and B. van Arem, "Rolling horizon control framework for driver assistance systems. Part II: Cooperative sensing and cooperative control," *Transp. Res. C, Emerg. Technol.*, vol. 40, pp. 290–311, Mar. 2014.
- [21] Y. Li, C. Tang, S. Peeta, and Y. Wang, "Nonlinear consensus-based connected vehicle platoon control incorporating car-following interactions and heterogeneous time delays," *IEEE Trans. Intell. Transp. Syst.*, vol. 20, no. 6, pp. 2209–2219, Jun. 2019.
- [22] Y. Li, C. Tang, S. Peeta, and Y. Wang, "Integral-Sliding-Mode braking control for a connected vehicle platoon: Theory and application," *IEEE Trans. Ind. Electron.*, vol. 66, no. 6, pp. 4618–4628, Jun. 2019.
- [23] F. Bu, H.-S. Tan, and J. Huang, "Design and field testing of a cooperative adaptive cruise control system," in *Proc. Amer. Control Conf.*, Jun. 2010, pp. 4616–4621.
- [24] Y. Li, C. Tang, K. Li, X. He, S. Peeta, and Y. Wang, "Consensus-based cooperative control for multi-platoon under the connected vehicles environment," *IEEE Trans. Intell. Transp. Syst.*, vol. 20, no. 6, pp. 2220–2229, Jun. 2019.
- [25] D. Chen, D. Sun, Y. Li, M. Zhao, and L. Zheng, "Robust stabilization and H ∞ control of cooperative driving system with time delay in variable speed-limited area from cyber-physical perspective," *Asian J. Control*, vol. 22, no. 1, pp. 373–387, 2020.
- [26] D. Chen, D. Sun, M. Zhao, L. Yang, T. Zhou, and F. Xie, "Distributed robust H ∞ control of connected eco-driving system with time-varying delay and external disturbances in the vicinity of traffic signals," *Nonlinear Dyn.*, vol. 92, no. 4, pp. 1829–1844, 2018.
- [27] K. Yu *et al.*, "Model predictive control for hybrid electric vehicle platooning using slope information," *IEEE Trans. Intell. Transp. Syst.*, vol. 17, no. 7, pp. 1894–1909, Jul. 2016.
- [28] J. Hu, Y. Shao, Z. Sun, M. Wang, J. Bared, and P. Huang, "Integrated optimal eco-driving on rolling terrain for hybrid electric vehicle with vehicle-infrastructure communication," *Transp. Res. C, Emerg. Technol.*, vol. 68, pp. 228–244, Jul. 2016.

- [29] C. Lei, E. M. van Eenennaam, W. K. Wolterink, G. Karagiannis, G. Heijenk, and J. Ploeg, "Impact of packet loss on CACC string stability performance," in *Proc. 11th Int. Conf. ITS Telecommun.*, Aug. 2011, pp. 381–386.
- [30] B. Besselink and K. H. Johansson, "String stability and a delay-based spacing policy for vehicle platoons subject to disturbances," *IEEE Trans. Autom. Control*, vol. 62, no. 9, pp. 4376–4391, Sep. 2017.
- [31] J. Ploeg, N. V. D. Wouw, and H. Nijmeijer, "Fault tolerance of cooperative vehicle platoons subject to communication delay," *IFAC-PapersOnLine*, vol. 48, no. 12, pp. 352–357, 2015.
- [32] W. Leutzbach, *Introduction to Theory Traffic Flow*, vol. 47. New York, NY, USA: Springer, 1988.
- [33] M. Wang, S. P. Hoogendoorn, W. Daamen, B. van Arem, B. Shyrokau, and R. Happee, "Delay-compensating strategy to enhance string stability of adaptive cruise controlled vehicles," *Transportmetrica B, Transp. Dyn.*, vol. 6, no. 3, pp. 211–229, Jul. 2018.
- [34] Y. Bai, Y. Zhang, and J. Hu, "Mobility oriented motion planning for cooperative lane changing under partially connected and automated environment," in *Proc. IEEE Int. Conf. Intell. Transp. Syst.*, 2018. [Online]. Available: <https://www.tandfonline.com/doi/abs/10.1080/23249935.2019.1645758?scroll=top&needAccess=true&journalCode=ttra21>
- [35] L. S. Pontryagin, *Mathematical Theory of Optimal Processes*. Boca Raton, FL, USA: CRC Press, 1987.
- [36] H. Moya-Cessa and F. Soto-Eguibar, *Differential Equations: An Operational Approach*. Princeton, NJ, USA: Rinton Press, 2011.
- [37] A. Boccia, L. Grüne, and K. Worthmann, "Stability and feasibility of state-constrained linear MPC without stabilizing terminal constraints," in *Proc. Int. Symp. Math. Theory Netw. Syst.*, 2014, pp. 453–460.
- [38] D. Swaroop and J. K. Hedrick, "String stability of interconnected systems," *IEEE Trans. Autom. Control*, vol. 41, no. 3, pp. 349–357, Mar. 1996.
- [39] D. Swaroop and J. K. Hedrick, "Constant spacing strategies for platooning in automated highway systems," *J. Dyn. Syst., Meas., Control*, vol. 121, no. 3, pp. 462–470, Sep. 1999.
- [40] E. Barbieri, "Stability analysis of a class of interconnected systems," *J. Dyn. Syst., Meas., Control*, vol. 115, no. 3, pp. 546–551, Sep. 1993.
- [41] K. Ahn, H. Rakha, A. Trani, and M. Van Aerde, "Estimating vehicle fuel consumption and emissions based on instantaneous speed and acceleration levels," *J. Transp. Eng.*, vol. 128, no. 2, pp. 182–190, Mar. 2002.
- [42] H. Rakha, K. Ahn, and A. Trani, "Development of VT-micro model for estimating hot stabilized light duty vehicle and truck emissions," *Transp. Res. D, Transp. Environ.*, vol. 9, no. 1, pp. 49–74, Jan. 2004.



Yu Zhang was born in Bazhong, Sichuan, China. He received the B.S. degree in traffic engineering from the Beijing Institute of Technology, Beijing, China, in 2016. He is currently pursuing the Ph.D. degree with Tongji University. His main research interests include connected and automated vehicle, optimal control theory, ITS, and eco-driving.



Yu Bai was born in Heilongjiang, China. She received the B.S. and Ph.D. degrees in traffic engineering from Tongji University, Shanghai, China, in 1999 and 2004, respectively. She has been with the College of Transportation Engineering, Tongji University, as an Assistant Professor from 2004 to 2012, as an Associate Professor from 2012 to 2019, and as a Professor since 2019. Her research interests include traffic design, traffic flow theory, and traffic safety.



Meng Wang (Member, IEEE) received the Ph.D. degree (*cum laude*) in transportation engineering from the Delft University of Technology (TU Delft), The Netherlands. He is currently an Assistant Professor and the Co-Director of the Electric and Automated Transport Research Lab, TU Delft. He has authored more than 80 publications in peer-reviewed journals and conferences. His main research interests are modeling, control design, and impact assessment of automated and cooperative driving systems for safe and efficient traffic flow operations. He serves as a member of the IEEE ITSS Technical Committee on Cooperative Driving and TRB Subcommittee on Traffic Flow Modeling for Connected and Automated Vehicles. He has received the IEEE ITS Society Best PhD Dissertation Award in 2015 and the IEEE ITSC Best Paper Award in 2013. He plays an active role in several research projects on automated driving and traffic management under the Dutch Automated Vehicle Initiative and EU Horizon 2020 Program. He is an Associate Editor of the IEEE TRANSACTIONS ON INTELLIGENT TRANSPORTATION SYSTEMS and has been the Associate Editors/IPC Members of the IEEE ITSS's flagship conferences of ITSC since 2013 and IV' since 2016.



Jia Hu (Member, IEEE) works as a ZhongTe Distinguished Chair in Cooperative Automation at the College of Transportation Engineering, Tongji University. Before joining Tongji, he was a Research Associate with the Federal Highway Administration, USA (FHWA). He is a member of TRB (a division of the National Academies) Vehicle Highway Automation Committee, Freeway Operation Committee, and Simulation Subcommittee of Traffic Signal Systems Committee, and a member of Advanced Technologies Committee of the ASCE Transportation and Development Institute. He is also the Chair of Vehicle Automation and Connectivity Committee of the World Transport Convention. He is an Associate Editor of the American Society of Civil Engineers *Journal of Transportation Engineering*, the IEEE OPEN JOURNAL IN INTELLIGENT TRANSPORTATION SYSTEMS, and an editorial board member of *International Journal of Transportation*.